# Cell Mechanic based on a centroidal void cylindrical Tensegrity Model to evaluate the Vibration of a Cellular Cytoskeleton

**Eiji Nouchi[1], Tomoteru Oka[2], Noriyuki Kataoka[3], Yoshihisa Kawano[4],**

***†Buntara S. Gan[1]**

[1]Department of Architecture, College of Engineering, Nihon University, Japan
[2]Department of Mechanical Engineering, Graduate School of Engineering, Nihon University, Japan
[3]Department of Mechanical Engineering, College of Engineering, Nihon University, Japan
[4]Department of Health Science, Faculty of Physical Education, International Pacific University, Japan

*Presenting author: gan.buntarasthenly@nihon-u.ac.jp
†Corresponding author: gan.buntarasthenly@nihon-u.ac.jp

## Abstract

Within the cytoplasm of a cell, there is a complex network of protein fibers that help maintain the cell's shape, secure some cells in specific positions, and allow cytoplasm and vesicles to move within the cell. These protein fibers enable cells within multicellular organisms to move. Collectively, this skeleton-like complex network of protein fibers is known as the Cellular Cytoskeleton in biology. There are many structural model hypotheses that scholars have proposed. However, there were constrained to the efforts of abstraction and conception to identify the mechanical behavior of the Cytoskeleton structure. Understanding the mechanical behavior of the Cytoskeleton is highly important to learn the important function of biological processes in a cell to heal humans from diseases by developing the appropriate medicines to cure the broken/infected cell. Moreover, many viruses' structures can be observed and identified from the cellular mechanical point of view. Sophisticated treatment methods to tame the viruses' activities could be discovered in the near future.

There are three types of filamentous proteins: filamentous actin (F-actin), intermediate filaments, and microtubules. The dynamic mechanism of a cellular cytoskeleton is essential for its role as a cell, and its accurate characterization has been a long-standing problem for cell scientists. A cytoskeleton's vibrations are highly influenced by interactions of filamentous proteins mediated by axial vibration of the stiff microtubules (compressive member) and lateral vibration of F-actin (tensile member). Among various structures in a cell, the cytoplasmic contractile bundles, Lamellipodia, and filipodia cells can be modeled by a symmetrical cylinder-shape self-equilibrium Tensegrity with different radii at the top and bottom of the cylinder. The truncated cone-like cylinder model is made to be small in height compared to the radii.

The tensegrity self-vibrational behavior of the Cytoskeleton is investigated to calculate the Cytoskeleton's natural frequencies, which are composed of the individual vibration of microtubules and F-actins experimental data. The Spectral Element Method based on the Wittrick-Williams procedure is adopted to solve the vibrational of the cellular Cytoskeleton. Various n-polygon cylindrical truncated cone-shaped skeletons to mimic the cytoskeletons are presented to demonstrate the robustness of the present study.

**Keywords:** Cell Mechanic, Tensegrity Structure, Vibration, Cytoskeleton, Spectral Element Method

## Introduction

Cells that makeup living organisms are exposed to various mechanical stimuli. In multicellular organisms, a network of cells forms a tissue. A system of tissues forms an organ [3,6,10,25]. Mechanical stimulation is involved in the background of cell morphology, motility, proliferation, and segregation and plays an important role in cell development and homeostasis. Inside a cell, there are organelles. Among the organelles, a cytoskeleton is a membrane that encloses the other organelles. The cellular cytoskeleton determines the cell's shape and triggers cell movement and form changes [1, 5, 19, 31-32, 35]. When receiving an external force, stress is generated in the intracellular cytoskeleton and cell adhesive apparatus. It has become clear that proteins constituting the cytoskeleton and cell adhesive apparatus, such as actin filaments (actin filaments), perceive mechanical stimuli. The actin scaffold undergoes mechanical stimulation in the cytoskeleton and is rapidly remodeled [47]. The role of this structure in mechanical response and its molecular mechanism has attracted attention [10,22,33,42,50-51]. Intermediate filaments have also been suggested to be involved in converting mechanical stimuli into chemical signals. However, although intermediate filaments are thought to play an important role in converting mechanical stimuli into chemical signals, the molecular mechanism remains unclear [1,8,14,21,34,44-45].

In recent years, there has been an idea that the structure of a cytoskeleton is in the form of a tensegrity structure [26-30]. Although tensegrity was originally used in the self-equilibrium concept in the field of structural mechanics, its structure is believed to be applied to the shape of a cell. The cytoskeleton comprises actin filaments, intermediate filaments, and microtubules, forming a three-dimensional filamentous structure inside the cell [11,23]. Microtubules in the cytoskeleton are rigid, and actin and intermediate filaments are elastic, indicating a specific composition of a tensegrity structure.

A tensegrity structure is a statically indeterminate structure composed of continuous cables, tensile members, and discontinuous struts, compressive members, composite structures [12-13,46]. Pins join these members, and the structure is in a self-equilibrium state without being supported. Many research results on tensegrity have been published in mechanics and architecture [15,38]. Various methods have been proposed in architecture for tensegrity structures' morphogenesis and their vibration characteristics [16,18,38-41,48].

In this study, as an initial attempt, we imitate the vibrational behaviors of a cytoskeleton by using a twisted and truncated n-plex cylindrical tensegrity structure. Fig. 1 illustrates the tensegrity model used to mimic the cytoskeleton structure. Sensitivity analyses are conducted to investigate the parameters that rule the vibrational behaviors of the cytoskeleton. In a real application, the parameters can be calibrated by using a result obtained from measurements of the real cytoskeleton.

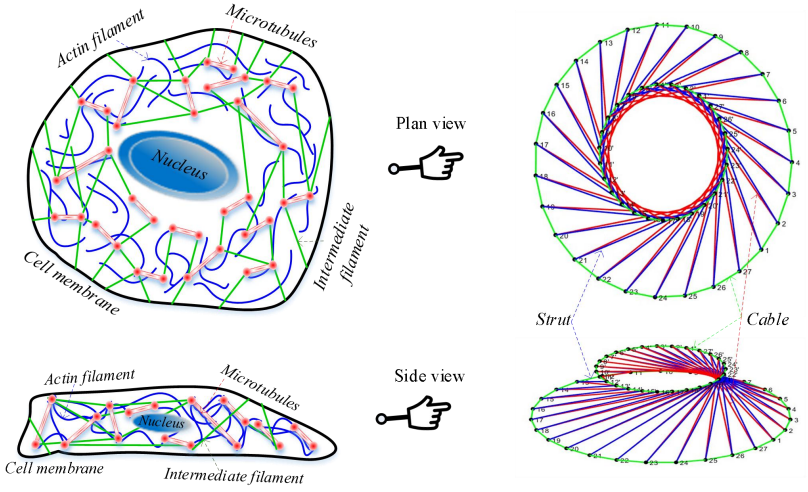

**Figure 1. A twisted cylindrical tensegrity model to mimic a cytoskeleton structure**

## Formulation of Tensegrity in Vibration

Fig. 2 shows a strut and a cable, two basic types of Tensegrity members. The compressive member strut and tensile member cable represent the microtubule and actin filament, respectively. The vibration of the strut is modeled as an axially vibrating microtubule of a cytoskeleton. At the same time, the cable's vibration is modeled to be a laterally vibrating actin filament of a cytoskeleton. The microtubule is presumed to have an axial rigidity represented by prestress force, P, and Young's modulus of elasticity, E. In contrast, the actin filament is presumed to have only an axial rigidity represented by prestress force, P.

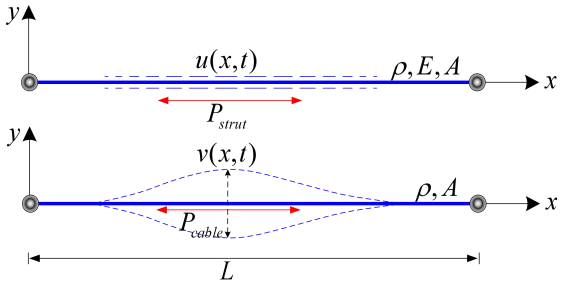


**Figure 2. Vibrational models of strut and cable members**

The equations of vibrational motion [2] are given as follows:

$$\begin{aligned} &\rho A\ddot{u} - \left(EA + P_{strut}\right)u'' = 0 \quad &&for\ strut \\ &\rho A\ddot{v} - P_{cable}v'' = 0 \quad &&for\ cable \end{aligned} \tag{1}$$

where, $u(x,t)$ and $v(x,t)$ are the axial and lateral displacements which are the function of position and time, respectively. The dot and prime superscripts denote the derivatives with respect to time $t$ and spatial coordinate $x$, respectively.

The internal forces and boundary conditions are given as,

$$\begin{aligned} &N(0,t) = -N_1(t),\ N(L,t) = N_2(t)\ or\ u(0,t) = u_1(t),\ u(L,t) = u_2(t) \quad &&for\ strut \\ &Q(0,t) = -Q_1(t),\ Q(L,t) = Q_2(t)\ or\ v(0,t) = v_1(t),\ v(L,t) = v_2(t) \quad &&for\ cable \end{aligned} \tag{2}$$

where $N(x,t), Q(x,t)$ are the axial and shear forces defined by,

$$\begin{aligned} N(x,t) &= \left(EA + P_{strut}\right)u'(x,t) \\ Q(x,t) &= P_{strut}v'(x,t) \end{aligned} \tag{3}$$

## Spectral Element Formulation

Analysis was performed using the Spectral Element Method (SEM) [1-2], a combination of the Finite Element Method (FEM), the Dynamic Stiffness Method (DSM), and the Spectral Analysis Method (SAM). The vibration of a tensegrity structure varies with the individual vibrational frequency and the wavelength of the members.

The FEM is a famous computational method used in many fields of engineering and science. However, it is difficult for the conventional FEM to analyze a structure such as a tensegrity

with no supporting boundaries, no external force, and a self-equilibrium state of the members. The DSM uses an exact dynamic stiffness matrix and implicitly considers the mass in the stiffness equation. The SAM uses the Fast Fourier Transform and has the property that the error converges exponentially if the solution is a smooth function ("exponential convergence"), converging much faster than the FEM. In spectral analysis, the dominant differential equation can be solved by infinitely adding waves with different frequencies and the time history of the solution that can be obtained from the Inverse Fourier Transform in the frequency-domain spectral components.
Fig. 3 depicts the concept of SEM as a combination of FEM, SAM, and SAM techniques in computing the vibration of Tensegrity structures.

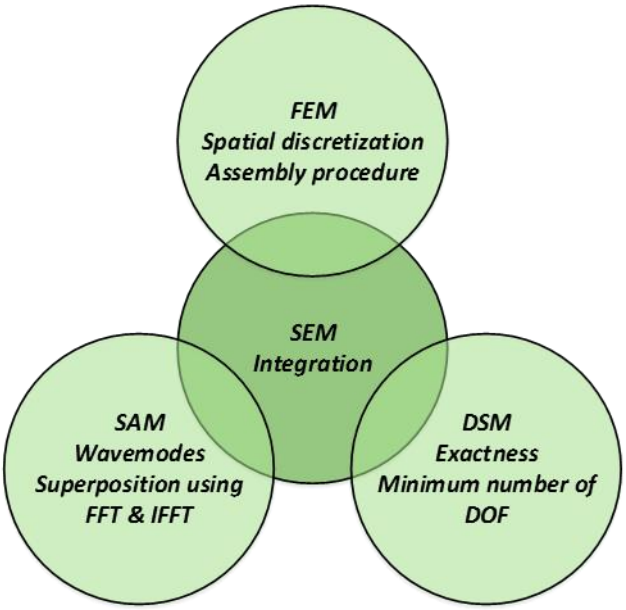


**Figure 3. Spectral Element Method (SEM) Outline**

*Governing equations in the frequency domain*

Assume the dynamic response of the Tensegrity in generalized coordinate $w(x,t)$, whereas in the spectral form given by,

$$w(x,t)=\frac{1}{M}\sum_{m=0}^{M-1}W_m(x)e^{i\omega_m t} \tag{4}$$

where $W_m(x)e^{i\omega_m t}$ is the generalized spectral components of the $u(x,t)$ or $v(x,t)$, $M$ is the sampling number, and $\omega_m$ is the $m^{th}$ natural frequency.

In spectral forms, the generalized boundary forces $F_1(t)$ and $F_2(t)$, the generalized boundary displacements $w_1(t)$ and $w_2(t)$ are also assumed to be as follows,

$$\{F_1(t),F_2(t)\}=\frac{1}{M}\sum_{m=0}^{M-1}\{F_{1m},F_{2m}\}e^{i\omega_m t} \tag{5}$$

$$\left\{w_1(t), w_2(t)\right\} = \frac{1}{M}\sum_{m=0}^{M-1}\left\{W_{1m}, W_{2m}\right\} e^{i\omega_m t} \tag{6}$$

*Spectral nodal Degree of Freedom (DOF) and Forces*

The spectral nodal generalized displacements $W(U,V)$ and forces $F(N,Q)$ are depicted in Fig. 4. Detail derivation of formulas can be found in [2]. Only relevant formulas are presented in the following.

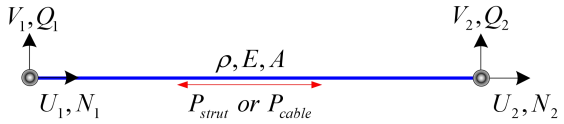


**Figure 4. Spectral nodal of generalized DOFs and Forces**

The spectral nodal DOFs vector is given by

$$\mathbf{d} = \left\{W_1 \quad W_2\right\}^T = \left\{W(0) \quad W(L)\right\}^T \tag{7}$$

and the spectral nodal forces vector is given by

$$\mathbf{f} = \left\{F_1 \quad F_2\right\}^T = \left\{-F(0) \quad +F(L)\right\}^T \tag{8}$$

*Dynamic shape function*

The solution of (4) can be given by,

$$W(x) = \sum_{r=1}^{2} a_r e^{-ik_r x} = \mathbf{e}(x;\omega)\boldsymbol{a} \tag{9}$$

where, the two wavenumbers can be determined by,

$$k_1 = +\omega\sqrt{\frac{\rho A}{P}} \quad and \quad k_2 = -\omega\sqrt{\frac{\rho A}{P}} \tag{10}$$

with $\mathbf{e}(x;\omega) = \left[e^{-ik_1 x} \quad e^{-ik_2 x}\right]$ and $\boldsymbol{a} = \left\{a_1 \quad a_2\right\}^T$.

The dynamic shape function can be obtained from,

$$W(x) = \mathbf{N}(x;\omega)\boldsymbol{a} \tag{11}$$

where $\mathbf{N}(x;\omega)$ is given by,

$$\mathbf{N}(x;\omega) = \mathbf{e}(x;\omega)\mathbf{H}_S^{-1}(\omega) = \frac{1}{e^{-ik_2 L} - e^{-ik_1 L}}\left[\left(e^{-i(k_2 L + k_1 x)} - e^{-i(k_1 L + k_2 x)}\right) \quad \left(-e^{-ik_1 x} + e^{-ik_2 x}\right)\right] \tag{12}$$

The spectral nodal DOFs vector of (7) can be formulated by substitution of (11) into (12),

which gives,

$$\mathbf{d} = \mathbf{H}_S(\omega)\boldsymbol{a} \tag{13}$$

where,

$$\mathbf{H}_S(\omega) = \begin{bmatrix} 1 & 1 \\ e^{-ik_1 L} & e^{-ik_2 L} \end{bmatrix}$$

*Weak form of governing equation*

The spectral element equation of Tensegrity structures can be given as,

$$\mathbf{S}(\omega)\mathbf{d} = \mathbf{0} \tag{14}$$

where,

$$\mathbf{S}(\omega) = \left(\mathbf{H}_S^{-1}(\omega)\right)^T \mathbf{D}(\omega)\mathbf{H}_S^{-1}(\omega) \tag{15}$$

with,

$$\mathbf{D}(\omega) = -P\mathbf{K}^T\mathbf{E}_S\mathbf{K} - \rho A\omega^2\,\mathbf{E}_S \tag{16}$$

The derivation of the dynamic shape function (12) can be written as,

$$\mathbf{N}'(x;\omega) = -i\mathbf{e}(x;\omega)\mathbf{K}\,\mathbf{H}^{-1}(\omega) \tag{17}$$

where,

$$\mathbf{K} = \begin{bmatrix} k_1 & 0 \\ 0 & k_2 \end{bmatrix}$$

$$\mathbf{E}_S(\omega) = \int_0^L \left[\mathbf{e}^T(x;\omega)\mathbf{e}(x;\omega)\right]dx = L$$

.

The Wittrick-Williams procedure is adopted to solve the natural vibrations of the cellular cytoskeleton based on the dynamic Tensegrity formulations above.

**Vibrational characteristic of Tensegrity**

Analysis was performed using the Spectral Element Method (SEM), which is a combination of the Finite Element Method (FEM), the Dynamic Stiffness Method (DSM), and the Spectral Analysis Method (SAM).

*Natural Vibrations of components of Tensegrity*

The vibration of a tensegrity structure is highly determined by the combination of vibrations of its components (cables and struts) behaviors. Physical data of each cytoskeleton component is obtained from the following literature.

- Length: Actin [3-6] = 3~20 μm (60 nm, unit length); Microtubule [4-6] = 10 μm
- Diameter: Actin [3-6] = 7~10 nm; Microtubule [3-6] = 25 nm

- Density: Actin [7] = 1.38~1.40 gram/cm$^3$; Microtubule [8] = 1.41 gram/cm$^3$
- Elastic modulus: Microtubule [8] = ~ 1 GPa

The tensions per unit length are obtained from the self-equilibrium equation in [1]. Table 1 shows the physical properties of 9-plex cytoskeleton components based on the literature.

**Table 1. Physical properties of 9-plex cytoskeleton components**

| Component | Microtubule (diagonal strut) | Actin-filament (top and bottom cables) | Actin-filament (diagonal cable) |
|---|---|---|---|
| Length (nm) | 1912.8 | 500.0 | 1711.1 |
| Diameter (nm) | 25 | 7 | 7 |
| Density (μg/nm$^3$) | 1.41e-15 | 1.38e-15 | 1.38e-15 |
| Elastic Modulus (Pa) | 3.0e-5 | - | - |
| Tension per unit length (aN/nm) | -2.736e-6 | 4.0e-8 | 2.736e-6 |

Figure 5 shows the model of a 9-plex cytoskeleton tensegrity structure and the results of natural frequencies that satisfy (14), as can be seen as drops in the logarithmic values of the determinant of dynamic stiffness. The first drop is called the structure's first mode of natural frequency.

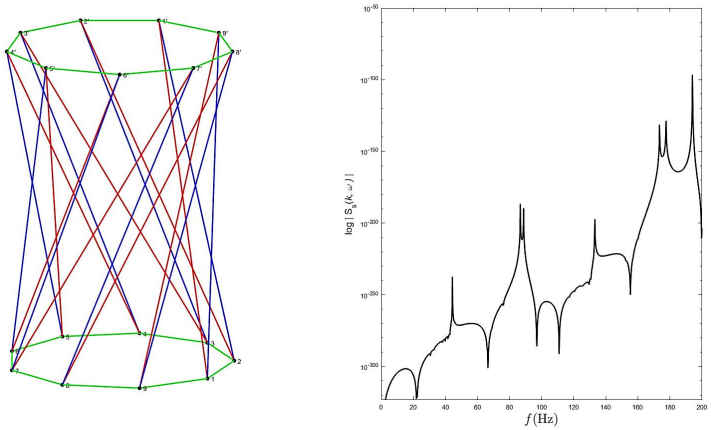


**Figure 5. Vibration of a 9-plex cytoskeleton tensegrity structure (1st mode: 21.963 Hz)**

Figure 6 shows natural frequency graphs of each component of the 9-plex cytoskeleton tensegrity structure.

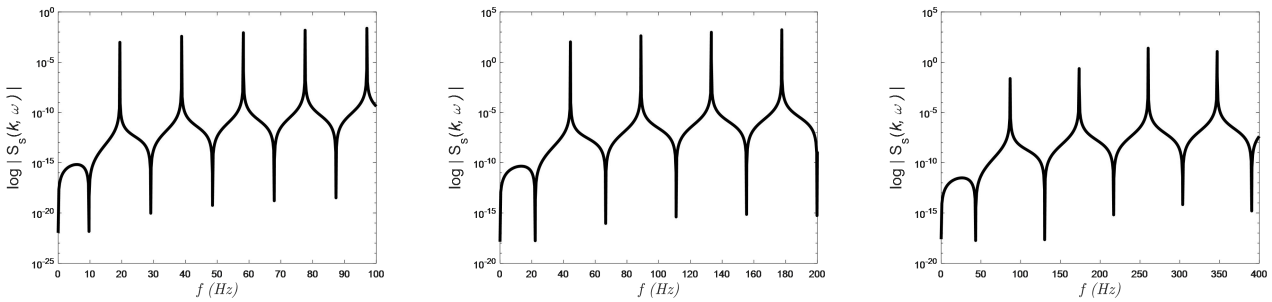


Top/bottom actin filament (9.704 Hz)

Microtubule (22.196 Hz)

Diagonal actin filament (43.381 Hz)

**Figure 6. The first five modes vibration of struts and cables in a 9-plex tensegrity cell**

*Height variation*

The variation of heights of the cytoskeleton structure is investigated in this section. Table 2 shows the height variation configurations of the tensegrity structures with their physical properties, which are required to compute the natural frequencies of the structures.

**Table 2. Physical properties of 9-plex tensegrities**

| Height (nm) | | 1193.2 ($0.2H_0$) | 894.94 ($0.6H_0$) | 1193.2 ($0.8H_0$) | 1491.6 ($1.0H_0$) |
|---|---|---|---|---|---|
| Length (nm) | Microtubule | 1234.1 | 1495.0 | 1690.5 | 1912.8 |
| | Actin top&bottom | 500.0 | | | |
| | Actin diagonal | 890.0 | 1226.4 | 1458.4 | 1711.1 |
| Diameter (nm) | Microtubule | 25 | | | |
| | Actin | 7 | | | |
| Density[3] ($\mu g/nm^3$) | Microtubule | 1.41e-15 | | | |
| | Actin | 1.38e-15 | | | |
| Elastic Modulus[6] | Microtubule | 3.0e-5 | | | |
| Tensile Coefficient (aN/nm) | Actin top (as reference) | 4.0e-6 | | | |

Figures 7-9 show the model of a 9-plex cytoskeleton tensegrity structure with height variations of 0.8H, 0.6H, and 0.2H, respectively. The first mode of natural frequencies of the various height cytoskeleton tensegrity structures that satisfy (14) can be seen at the first drops in the logarithmic values of the determinant of dynamic stiffness.

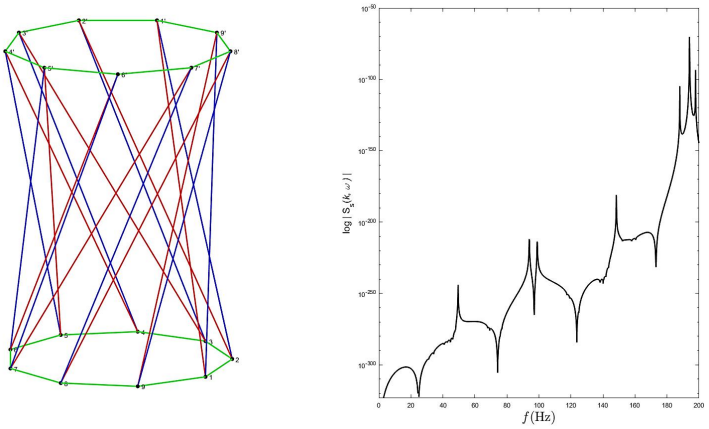


**Figure 7. Vibration of a 9-plex tensegrity cell (0.8H = 25.000 Hz)**

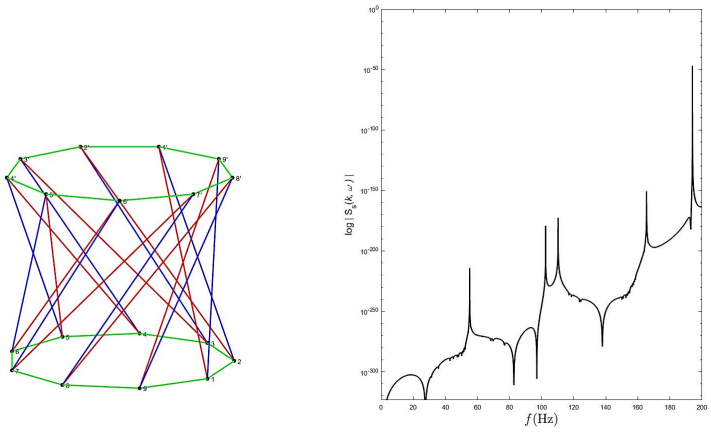


**Figure 8. Vibration of a 9-plex tensegrity cell (0.6H = 27.399 Hz)**

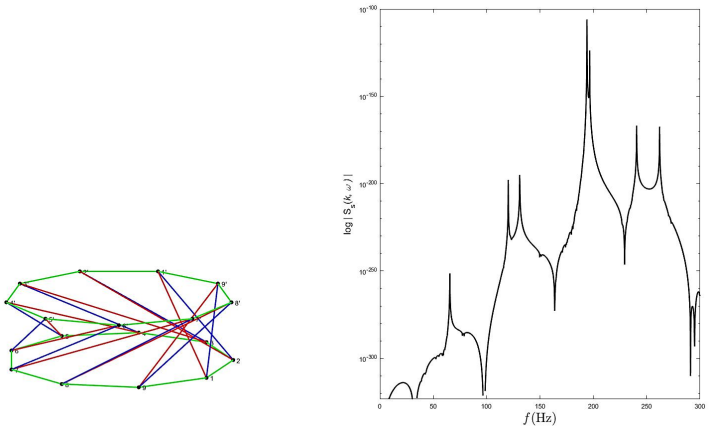


**Figure 9. Vibration of a 9-plex tensegrity cell (0.2H = 30.240 Hz)**

*n-plex variation*

This section investigates the variation of 0.2H height of n-plex cytoskeleton twisted cylindrical tensegrity structures. Table 3 shows the physical properties of 9, 12, and 15-plex cytoskeleton tensegrity structures, respectively.

**Table 3. Physical properties of *n*-plex tensegrities**

| *n*-Plex | | 9 | 12 | 15 |
|---|---|---|---|---|
| Height (nm) | | | 20.24 (*1.4%* $H_0$) | |
| Length (nm) | Microtubule | 1847.3 | 1950.2 | 2482.7 |
| | Actin top&bottom | | 500&1000 | |
| | Actin diagonal | 1396.7 | 2394.8 | 2927.2 |
| Diameter (nm) | Microtubule | | 25 | |
| | Actin | | 7 | |
| Density[3] (μg/nm$^3$) | Microtubule | | 1.41e-15 | |
| | Actin | | 1.38e-15 | |
| Elastic Modulus[6] (Pa) | Microtubule | | 3.0e+9 | |
| Tensile Coefficient (aN/nm) | Actin top (as refere | | 4.0e-6 | |

Figures 10-12 show the model of an *n*-plex cytoskeleton tensegrity structure with 0.2H of height. The first mode of natural frequencies of the *n*-plex cytoskeleton tensegrity structures that satisfy (14) can be seen at the first drops in the logarithmic values of the determinant of dynamic stiffness.

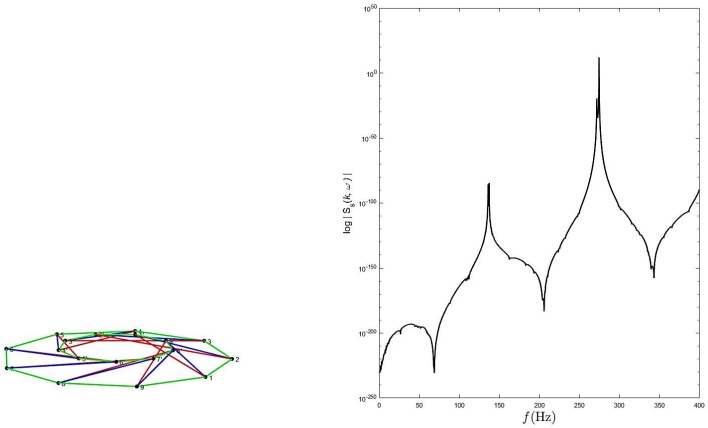


**Figure 10. Vibration of a truncated 9-plex conic tensegrity cell ($f_1$ = 68.61 Hz)**

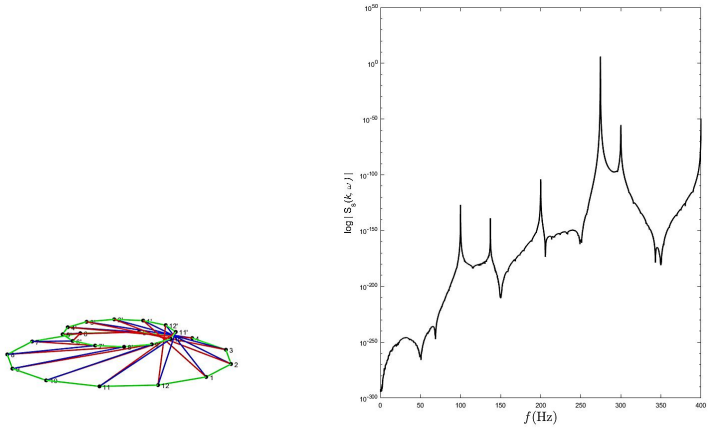


**Figure 11. Vibration of a truncated 12-plex conic tensegrity cell ($f_1$ = 50.61 Hz)**

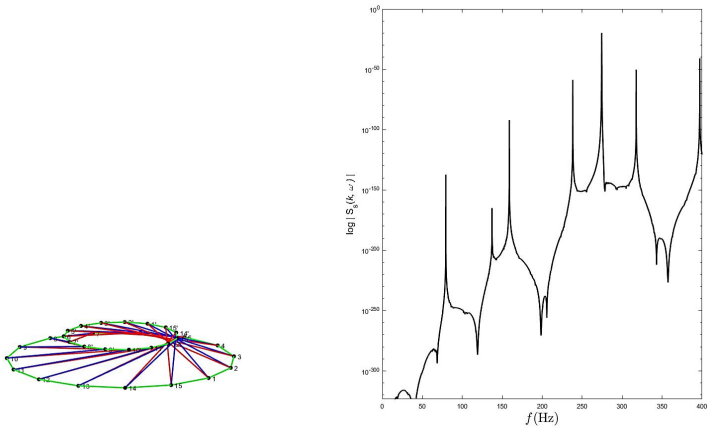


**Figure 12. Vibration of a truncated 15-plex conic tensegrity cell ($f_1$ = 35.49 Hz)**

## Summary and conclusion

In Figs. 5-6, we can observe that the cellular 9-plex tensegrity has the 1st mode natural frequency, which is close to the 1st mode natural frequency of its strut (Microtubule) because the actin filaments are assumed to vibrate in their lateral direction. In contrast, the microtubule is assumed to vibrate in its axial direction, controlling the vibrational behaviors of the tensegrity.

The height of 9-plex tensegrity is varied by 0.8, 0.6, and 0.2 times the height H. Figs. 7-9 show that the 1st mode of their natural frequency was increasing by reducing the height.

Fixing the height of the 9-plex tensegrity with the 0.2H height, the 1st modes of the 12- and 15-plex tensegrity show the reduction of natural frequency since they become stiffer than the 9-plex tensegrity.

By using tensegrity, we obtained physical properties to reproduce the fluctuations of cells. In the future, we will investigate the significance of fluctuations in the cellular structure composed of actin filaments and microtubules subjected to traction force by observing them under different temperatures and mechanical conditions and by approximating the shape of actual cells. Also, this time, we reproduced the cell shape using a cylindrical model, but since the actual cell has a complicated shape, it is necessary to use random numbers and precise modeling of the cytoskeleton structure for verification. Further elucidation of the molecular mechanism of cytoskeletal control by mechanical stimulation received by cells is expected by developing techniques that can measure the force and shape of the cytoskeleton.

All the cells that make up our body receive mechanical stimuli and maintain homeostasis through appropriate haptic responses. Its failure is expected to be the cause of many diseases. By advancing the elucidation of the process by which cells receive mechanical stimuli and transform them into chemical signals, many discoveries have been made about problems that could not be explained only by chemical signals. It is expected that it will be useful in investigating mechanical cell behaviors.

## Conflicts of Interest

The authors declare no conflict of interest.

## Declaration of generative AI

The authors declare the the present work has no AI generated products.

### References


[1] G. Albrecht-Buehler, Role of cortical tension in fibroblast shape and movement., Cell Motil. Cytoskeleton. 7 (1987) 54–67. https://doi.org/10.1002/cm.970070108.

[2] J.R. Banerjee, Dynamic stiffness formulation for structural elements: A general approach, Comput. Struct. 63 (1997) 101–103. https://doi.org/10.1016/S0045-7949(96)00326-4.

[3] T. Barata, V. Vieira, R. Rodrigues, R.P. das Neves, M. Rocha, Reconstruction of tissue-specific genome-scale metabolic models for human cancer stem cells, Comput. Biol. Med. 142 (2022). https://doi.org/10.1016/j.compbiomed.2021.105177.

[4] D.E. Beskos, G. V. Narayanan, Dynamic response of frameworks by numerical laplace transform, Comput. Methods Appl. Mech. Eng. 37 (1983) 289–307. https://doi.org/10.1016/0045-7825(83)90080-4.

[5] M.E. Chicurel, C.S. Chen, D.E. Ingber, Cellular control lies in the balance of forces, Curr. Opin. Cell Biol. 10 (1998) 232–239. https://doi.org/10.1016/S0955-0674(98)80145-2.

[6] D.W. Deamer, The origin of cellular life, Planets Life Emerg. Sci. Astrobiol. 22 (2007) 187–210. https://doi.org/10.1017/cbo9780511812958.011.

[7] B. Demé, D. Hess, M. Tristl, L.T. Lee, E. Sackmann, Binding of actin filaments to charged lipid monolayers: Film balance experiments combined with neutron reflectivity, Eur. Phys. J. E. 2 (2000) 125–136. https://doi.org/10.1007/s101890050046.

[8] C. Dong, R. Skalak, K.L.P. Sung, Cytoplasmic rheology of passive neutrophils, Biorheology. 28 (1991) 557–567. https://doi.org/10.3233/BIR-1991-28607.

[9] J.F. Doyle, Wave Propagation in Structures, Wave Propag. Struct. (1989) 126–156. https://doi.org/10.1007/978-1-4684-0344-2_6.

[10] J. Feher, Cell Structure, Quant. Hum. Physiol. (2017) 101–119. https://doi.org/10.1016/b978-0-12-800883-6.00010-0.
[11] E.G. Fey, K.M. Wan, S. Penman, Epithelial cytoskeletal framework and nuclear matrix-intermediate filament scaffold: three-dimensional organization and protein composition, J. Cell Biol. 98 (1984) 1973–1984. https://doi.org/10.1083/jcb.98.6.1973.
[12] Fuller, Tensegrity, Portf. Artnews Annu. (1961) 112–127.
[13] R.B. Fuller, Conceptuality of Fundamental Structures, 1965. https://books.google.co.jp/books?id=HEL6NwAACAAJ.
[14] Y.C. Fung, S.Q. Liu, Elementary mechanics of the endothelium of blood vessels, J. Biomech. Eng. 115 (1993) 1–12. https://doi.org/10.1115/1.2895465.
[15] H. Furuya, Concept of Deployable Tensegrity Structures in Space Application, Int. J. Sp. Struct. 7 (1992) 143–151. https://doi.org/10.1177/026635119200700207.
[16] B.S. Gan, Self-vibrational Analysis of a Tensegrity, in: N. Tien Khiem, T. Van Lien, N. Xuan Hung (Eds.), Lect. Notes Mech. Eng., Springer Singapore, Singapore, 2022: pp. 87–99. https://doi.org/10.1007/978-981-16-3239-6_7.
[17] B.S. Gan, Computational Modeling of Tensegrity Structures: Art, Nature, Mechanical and Biological Systems, Springer Cham, 2019. https://doi.org/10.1007/978-3-030-17836-9.
[18] B.S. Gan, J. Zhang, D.K. Nguyen, E. Nouchi, Node-based genetic form-finding of irregular tensegrity structures, Comput. Struct. 159 (2015) 61–73. https://doi.org/10.1016/j.compstruc.2015.07.003.
[19] M.L. Gardel, K.E. Kasza, C.P. Brangwynne, J. Liu, D.A. Weitz, Chapter 19 Mechanical Response of Cytoskeletal Networks, Methods Cell Biol. 89 (2008) 487–519. https://doi.org/10.1016/S0091-679X(08)00619-5.
[20] E. Ghavanloo, F. Daneshmand, M. Amabili, Vibration analysis of a single microtubule surrounded by cytoplasm, Phys. E Low-Dimensional Syst. Nanostructures. 43 (2010) 192–198. https://doi.org/10.1016/j.physe.2010.07.016.
[21] F. Gittes, B. Mickey, J. Nettleton, J. Howard, Flexural rigidity of microtubules and actin filaments measured from thermal fluctuations in shape, J. Cell Biol. 120 (1993) 923–934. https://doi.org/10.1083/jcb.120.4.923.
[22] D.C. Haspinger, S. Klinge, G.A. Holzapfel, Numerical analysis of the impact of cytoskeletal actin filament density alterations onto the diffusive vesicle-mediated cell transport, PLoS Comput. Biol. 17 (2021) 1–26. https://doi.org/10.1371/journal.pcbi.1008784.
[23] J.E. Heuser, M.W. Kirschner, Filament organization revealed in platinum replicas of freeze-dried cytoskeletons, J. Cell Biol. 86 (1980) 212–234. https://doi.org/10.1083/jcb.86.1.212.
[24] M. Igaev, H. Grubmüller, Microtubule instability driven by longitudinal and lateral strain propagation, PLoS Comput. Biol. 16 (2020) 1–21. https://doi.org/10.1371/journal.pcbi.1008132.
[25] D.E. Ingber, Cellular tensegrity: Defining new rules of biological design that govern the cytoskeleton, J. Cell Sci. 104 (1993) 613–627. https://doi.org/10.1242/jcs.104.3.613.
[26] D.E. Ingber, J.D. Jamieson, Tumor formation and malignant invasion: role of basal lamina, in: L.A. Liotta, I.R. Hart (Eds.), Tumor Invasion and Metastasis, Springer Netherlands, Dordrecht, 1982: pp. 335–357. https://doi.org/10.1007/978-94-009-7511-8_20.
[27] D.E. Ingber, J.A. Madri, J.D. Jamieson, Role of basal lamina in neoplastic disorganization of tissue architecture, Proc. Natl. Acad. Sci. U. S. A. 78 (1981) 3901–3905. https://doi.org/10.1073/pnas.78.6.3901.
[28] D.E. Ingber, Tensegrity I. Cell structure and hierarchical systems biology, J. Cell Sci. 116 (2003) 1157–1173. https://doi.org/10.1242/jcs.00359.
[29] D.E. Ingber, The riddle of morphogenesis: A question of solution chemistry or molecular cell engineering?, Cell. 75 (1993) 1249–1252. https://doi.org/10.1016/0092-8674(93)90612-T.
[30] D.E. Ingber, Tensegrity II. How structural networks influence cellular information processing networks, J. Cell Sci. 116 (2003) 1397–1408. https://doi.org/10.1242/jcs.00360.
[31] D.E. Ingber, L. Dike, L. Hansen, S. Karp, H. Liley, A. Maniotis, H. McNamee, D. Mooney, G. Plopper, J. Sims, N. Wang, Cellular Tensegrity: Exploring How Mechanical Changes in the Cytoskeleton Regulate Cell Growth, Migration, and Tissue Pattern during Morphogenesis, Int. Rev. Cytol. 150 (1994) 173–224. https://doi.org/10.1016/S0074-7696(08)61542-9.
[32] D.E. Ingber, D. Prusty, Z. Sun, H. Betensky, N. Wang, Cell shape, cytoskeletal mechanics, and cell cycle control in angiogenesis, J. Biomech. 28 (1995) 1471–1484. https://doi.org/10.1016/0021-9290(95)00095-X.
[33] V.V.S.V. Jakka, J. Bursa, Impact of physiological loads of arterial wall on nucleus deformation in endothelial cells: A computational study, Comput. Biol. Med. 143 (2022) 105266. https://doi.org/10.1016/j.compbiomed.2022.105266.

[34] P.A. Janmey, U. Euteneuer, P. Traub, M. Schliwa, Viscoelastic properties of vimentin compared with other filamentous biopolymer networks, J. Cell Biol. 113 (1991) 155–160. https://doi.org/10.1083/jcb.113.1.155.
[35] P.A. Janmey, The cytoskeleton and cell signaling: Component localization and mechanical coupling, Physiol. Rev. 78 (1998) 763–781. https://doi.org/10.1152/physrev.1998.78.3.763.
[36] U. Lee, Spectral Element Method in Structural Dynamics, John Wiley & Sons (Asia) Pte Ltd, 2009. https://doi.org/10.1002/9780470823767.
[37] A.Y.T. Leung, Dynamic Stiffness and Substructures, Springer-Verlag, 1993. https://doi.org/10.1007/978-1-4471-2026-1.
[38] P. Motro, R., Najari, S., Jouanna, Tensegrity systems. From design to realization., in: Proc. First Int. Conf. Light. Struct. Archit., 1986.
[39] B. Moussa, N. Ben Kahla, J.C. Pons, Evolution of natural frequencies in tensegrity systems: A case study, Int. J. Sp. Struct. 16 (2001) 57–73. https://doi.org/10.1260/0266351011495322.
[40] H. Murakami, Static and dynamic analyses of tensegrity structures. Part 1. Nonlinear equations of motion, Int. J. Solids Struct. 38 (2001) 3599–3613. https://doi.org/10.1016/S0020-7683(00)00232-8.
[41] I.J. Oppenheim, W.O. Williams, Vibration of an elastic tensegrity structure, Eur. J. Mech. A/Solids. 20 (2001) 1023–1031. https://doi.org/10.1016/S0997-7538(01)01181-0.
[42] A.F. Pegoraro, P. Janmey, D.A. Weitz, Mechanical properties of the cytoskeleton and cells, Cold Spring Harb. Perspect. Biol. 9 (2017). https://doi.org/10.1101/cshperspect.a022038.
[43] J. Pokorný, F. Jelínek, V. Trkal, I. Lamprecht, R. Hölzel, Vibrations in Microtubules, J. Biol. Phys. 23 (1997) 171–179. https://doi.org/10.1023/A:1005092601078.
[44] G.W. Schmid-Schönbein, T. Kosawada, R. Skalak, S. Chien, Membrane model of endothelial cells and leukocytes. A proposal for the origin of a cortical stress, J. Biomech. Eng. 117 (1995) 171–178. https://doi.org/10.1115/1.2795999.
[45] G.C. Sieck, Controversies in physiology, J. Appl. Physiol. 89 (2000) 407. https://doi.org/10.1152/jappl.2000.89.2.407.
[46] K. Snelson, Snelson on the tensegrity invention, Int. J. Sp. Struct. 11 (1996) 43–48. https://doi.org/10.1177/026635119601-207.
[47] D. Stamenović, D.E. Ingber, Models of cytoskeletal mechanics of adherent cells, Biomech. Model. Mechanobiol. 1 (2002) 95–108. https://doi.org/10.1007/s10237-002-0009-9.
[48] C. Sultan, M. Corless, R.E. Skelton, Linear dynamics of tensegrity structures, Eng. Struct. 24 (2002) 671–685. https://doi.org/10.1016/S0141-0296(01)00130-4.
[49] A. Tounsi, H. Heireche, H. Benhassaini, M. Missouri, Vibration and length-dependent flexural rigidity of protein microtubules using higher order shear deformation theory, J. Theor. Biol. 266 (2010) 250–255. https://doi.org/10.1016/j.jtbi.2010.06.037.
[50] Y. Ujihara, M. Nakamura, M. Soga, K. Koshiyama, H. Miyazaki, S. Wada, Computational studies on strain transmission from a collagen gel construct to a cell and its internal cytoskeletal filaments, Comput. Biol. Med. 56 (2015) 20–29. https://doi.org/10.1016/j.compbiomed.2014.10.015.
[51] P. Urdeitx, S.J. Mousavi, S. Avril, M.H. Doweidar, Computational modeling of multiple myeloma interactions with resident bone marrow cells, Comput. Biol. Med. 153 (2023) 106458. https://doi.org/10.1016/j.compbiomed.2022.106458.
[52] W.H. Wittrick, F.W. Williams, A general algorithm for computing natural frequencies of elastic structures, Q. J. Mech. Appl. Math. 24 (1971) 263–284. https://doi.org/10.1093/qjmam/24.3.263.